

Strain and Temperature Characterization of LPGs Written by CO₂ Laser in Pure Silica LMA Photonic Crystal Fibers

Roberta Cardoso CHAVES^{1*}, Alexandre de Almeida Prado POHL¹, Ilda ABE²,
Renan SEBEM³, and Aleksander PATERNO³

¹Laboratório Avançado de Telecomunicações, Federal University of Technology, Paraná, Brazil

²Laboratório de Fotônica, Federal University of Technology, Paraná, Brazil

³Laboratory of Optoelectronic Systems, Santa Catarina State University, Santa Catarina, Brazil

*Corresponding author: Roberta Cardoso CHAVES E-mail: robbychaves@gmail.com

Abstract: This paper reports on the writing of long period gratings (LPGs) in a six-ring pure silica solid core, and large mode area photonic crystal fiber (fiber core diameter $\rho = 10.1 \mu\text{m}$) using a CO₂ laser system, and the characterization of their strain and temperature sensitivities. Temperature and strain sensitivities in the order of $-19.6 \text{ pm}/^\circ\text{C}$ and $-88 \text{ pm}/\mu\epsilon$, respectively, were obtained, which were comparable or surpassed values of the similar photonic crystal fiber (PCF)-based LPG or sensor configurations found in the literature.

Keywords: Long period grating, photonic crystal fiber, CO₂ laser

Citation: Roberta Cardoso CHAVES, Alexandre de Almeida Prado POHL, Ilda ABE, Renan SEBEM, and Aleksander PATERNO, "Strain and Temperature Characterization of LPGs Written by CO₂ Laser in Pure Silica LMA Photonic Crystal Fibers," *Photonic Sensors*, 2015, 5(3): 241–250.

1. Introduction

Photonic crystal fiber (PCF), also called microstructured optical fiber (MOF), is a type of optical fiber with a microstructured cladding, which improves some light propagation features and even introduces new ones when compared to the properties of conventional optical fibers [1, 2]. For example, they operate as single mode optical waveguides over a broad range of wavelengths [3]; they present lower bend losses [4]; they enable specific designs for the exploitation of nonlinearities [5], and they can also guide light in hollow cores [6]. This class of optical fiber is characterized by a particular set of design parameters, such as the diameter, d , of the air holes in the cladding, core

diameter, ρ , and pitch, A_{PCF} , that allows one to design the fiber for specific operational purposes. Moreover, sensing with PCFs provides a new way of measuring physical parameters, such as pressure and temperature, and also chemical compounds, among others. For instance, the holes in the cladding can also be filled with proper liquids or gases providing increased sensitivity of measurands [7, 8].

Several fabrication methods, such as ultraviolet (UV) laser exposure [9], CO₂ laser irradiation [10, 11], and femtosecond laser exposure [12], have been employed to write long period fiber gratings (LPGs) in solid core photonic crystal fibers. The CO₂ laser irradiation technique is more flexible and offers lower cost as no phase masks and no special photosensitive fiber are required to write the grating,

Received: 3 March 2015 / Revised version: 2 June 2015

© The Author(s) 2015. This article is published with open access at Springerlink.com

DOI: 10.1007/s13320-015-0250-3

Article type: Regular

as compared to the UV laser exposure technique. In addition, the CO₂ laser irradiation process can be controlled via the point-by-point inscription technique to generate complex grating profiles. In this way, the use of CO₂ laser for writing LPGs in PCFs is one of the most adequate and flexible methods to obtain good quality gratings.

Basically, LPGs couple light between the fundamental core mode and forward propagating cladding modes, leading to dips in the transmission spectrum, at wavelengths that match the resonant condition. In this way, their properties are different from those of fiber Bragg gratings (FBGs) that work in reflection. Given that pure silica PCFs are made fundamentally of one single material, LPGs written in such fibers present different strain and temperature sensitivities as compared to gratings in conventional fibers due to the fact that these are composed of at least two different glasses showing different thermal expansion coefficients [11]. In this way, PCF-based LPGs can even be temperature insensitive and have attracted particular attention because of their potential for realizing temperature-insensitive sensors [13, 14], as well as for achieving stable optical band rejection filters [15, 16] and gaining equalizers [17] without requiring any complex packaging. Furthermore, as devices written in fibers, PCF-based-LPGs present low insertion loss, immunity to electromagnetic interference and have small dimensions, which is of advantage for compact and miniaturized sensors on demand in industrial environments.

The growth of the LPG depends on features like the duration of the exposure to the laser beam, the laser power, the period, and the length of the grating [11]. The last one, the length of the grating, is given by $L=(N*\Lambda)$, where N is the number of points of the fiber reached by the laser beam, and Λ is the period of the LPG. Given the increasing importance of PCF-based LPGs for several sensing applications, this work described their fabrication using the CO₂ laser irradiation exposure in a commercial six-ring

solid core, pure silica, large mode area photonic crystal fiber, and their characterizations over strain and temperature in order to obtain the corresponding sensitivity. It is not necessary to hydrogenate the PCF fiber in order to increase its photosensitivity. The data are compared with results from the literature and contribute to the amount of information required for the design and fabrication of improved sensors in photonic crystal fibers.

2. Writing of PCF-based long period gratings

The large mode area PCF from NKT Photonics (LMA-10) with the core diameter $\rho = 10.1 \mu\text{m}$, hole diameter $d = 2.95 \mu\text{m}$, and pitch $\Lambda_{\text{PCF}}=6.9 \mu\text{m}$ was employed in this work. The fiber had a pure silica core and six rings of air holes surrounding the core. The fiber was single mode over a large range of optical wavelengths, and its cross section is shown in Fig. 1.

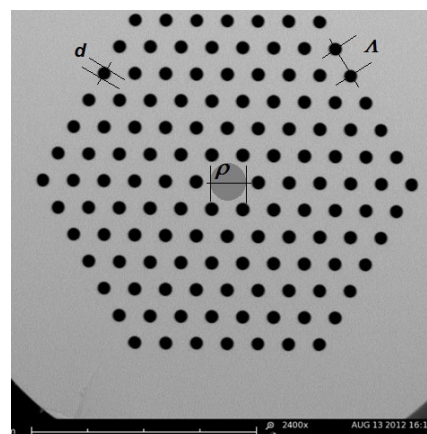


Fig. 1 Optical microscopy photograph of the cleaved end of the LMA-10 (the microstructure cladding consists of air holes with the diameter $d=2.95 \mu\text{m}$ arranged in a triangular lattice with the spatial pitch Λ_{PCF} ; the solid silica core is formed by the “missing” air hole indicated by the gray circle with the diameter ρ).

Samples of the LMA-10 were spliced to the standard single mode fiber (SMF) at its two ends using a fusion splicer (FSM-50S, Fujikura) by controlling the splicer parameters in order to reduce splice losses. Optimal splicing has occurred when the PCF mode field diameter was enlarged and matched the corresponding SMF mode field

diameter at the interface. The average loss obtained was 1.5 dB/splice. The employed CO₂ laser (Coherent – Diamond C30A) had a nominal power of 30 W and was set to operate at a repetition rate of 5 kHz. A micro-controller produced a pulse-width modulating signal that drove the laser to the desired output power. To write gratings, the power of the laser, P , and the fiber exposition time, t , were set in the computer controlled laser system. This system is very flexible, allowing a large variation of the writing parameters in order to customize devices. Light from an amplified spontaneous emission (ASE) source was launched into the fiber with the purpose of monitoring the transmission spectrum during the fabrication process with an optical spectrum analyzer (OSA). A ZnSe cylindrical lens (ULO Optics) with a focal length of 100 mm was used to collimate the CO₂ beam on the fiber. A weight of 13 g was attached to the loose fiber end on a fixed translator stage, keeping the fiber under tension during the imprinting process. The other end of the fiber was fixed on a V-groove with a fiber holder, which was pulled by a motorized translation stage. By employing the point-by-point technique, this stage was configured to stop at every point of the desired LPG period in order for the laser to shoot a train of pulses on the fiber. Figure 2 shows a diagram of the experimental setup, which is similar to that used by Yang *et al.* [18]. Some parameters were kept constant during the writing process. For instance, the duty cycle of the PWM for the CO₂ laser was set to 30% of the available maximum, and the fiber exposition time t to the laser beam was adjusted to 150 ms. The number of points N and the pitch Λ of the LPG were changed over several writing sequences in order to write different gratings. Only one scan of the irradiation beam over the fiber was used to write the gratings.

As the laser pulses hit the fiber, the local heating causes the collapse of the holes in the cladding region, and a periodic disturbance along the guide as the motorized stage is moved along. By proper

adjustment of two parameters (e.g., the power of the laser and the exposure time), it is possible to control the size of the collapsed region in the fiber. Figure 3 shows a picture of the region, in which the laser has modified the fiber structure.

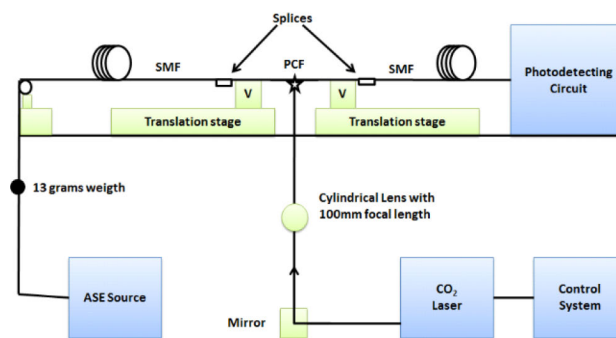


Fig. 2 Schematic of the experimental setup for writing PCF-based LPGs.

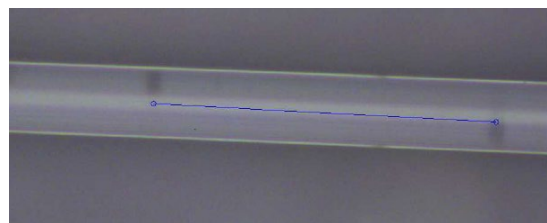


Fig. 3 Optical microscope photography of an irradiated area of the fiber, showing the markings produced by the CO₂ laser pulses.

Basically, three mechanisms account for the modulation of the refractive index in CO₂ laser-induced LPGs: residual stress relaxation, glass densification and/or physical deformation of the fiber [11]. Although no further efforts were pursued, within the scope of this work, to find out the primary mechanism for the refractive index change, evidences from other works in photonic crystal fibers [19–23] point out two main reasons: (a) the partial or complete collapse of air holes in the cladding, based on the mechanism known as “self-regulating” resulting from constant axial tension and (b) the local high-temperature induced by the laser pulses, as the main contribution to the refractive indices modification.

The transmission spectra of four LPGs imprinted on the LMA-10 PCF and identified by labels A, B, C, and D, are shown in Fig. 4. The periods of LPG-A,

LPG-B, LPG-C, and LPG-D were $A_A = 350 \mu\text{m}$, $A_B = 380 \mu\text{m}$, $A_C = 390 \mu\text{m}$, and $A_D = 400 \mu\text{m}$, respectively. The number of points N of each LPG was determined by stopping the writing process to preserve the observed resonance at the minimum transmission. For LPG-A, $N=3$; for LPG-B, the number of points was $N=17$; for LPG-C, $N=12$, and for LPG-D, $N=17$. These four samples presented peak resonance wavelengths at $\lambda_A = 1563 \text{ nm}$, $\lambda_B = 1547.6 \text{ nm}$, $\lambda_C = 1543.5 \text{ nm}$, and $\lambda_D = 1541 \text{ nm}$, respectively. The full widths at half maximum (FWHM) for each sample, illustrated by the horizontal line segments in Fig. 4, were measured as 4.1 nm, 1.4 nm, 1.8 nm, and 6.1 nm for LPGs A, B, C, and D, respectively. These gratings were used for the strain characterization study. LPG-A presented an FWHM of 4.1 nm and a total length of $L=1.05 \text{ mm}$. For comparison purposes with data found in the literature, the grating fabricated by Zhu *et al.* [23] presented an FWHM of 0.7 nm in a 2.8-mm-length LPG.

It can be observed from Fig. 4 that the insertion losses for LPGs A, B, C, and D imprinted on LMA-10 PCF are more than 10 dB. This can be due to the experimental setup used to write the gratings and can be reduced in future works. In that setup as illustrated in Fig. 2, the right end of the PCF fiber was fixed on a V-groove fiber holder, and it moved with the translation stage. The left end of the PCF fiber was free and maintained stretched only by a 13 g weight. At each shot of pulses from CO₂ laser beam, the 13 g weight swinging caused a fiber displacement, and the CO₂ laser beam could reach the PCF fiber not exactly perpendicularly. Because of that inclination, the train of pulses could collapse a larger number of air holes from microstructured cladding PCF fiber, causing higher losses.

Moreover, PCF fiber was spliced between two samples of SMF fiber, also illustrated in Fig. 2. The splice in the right end of the PCF fiber held in a V-groove did not suffer the effects produced by the 13 g weight. In the other hand, the left end of the

PCF fiber was free over the translation stage, and it was tensioned full time by a 13 g weight. That could cause misalignment between the PCF and SMF mode field diameters, also increasing insertion losses. These losses could be decreased by using not one, but two translations stages that moved at each shot of CO₂ laser pulses. In this way, both ends of the PCF fiber would be hold in a V-groove holder, avoiding the displacement and misalignment problems.

Two other samples were written with the CO₂ laser system in order to characterize their temperature sensitivity: LPG-E and LPG-F. Figure 5 shows the transmission spectra of such gratings. The numbers of points N of both two samples were set to be 20 in order to provide a contact length approximately equal for both gratings when placed over the Peltier junction element, since they had approximately the same period Λ .

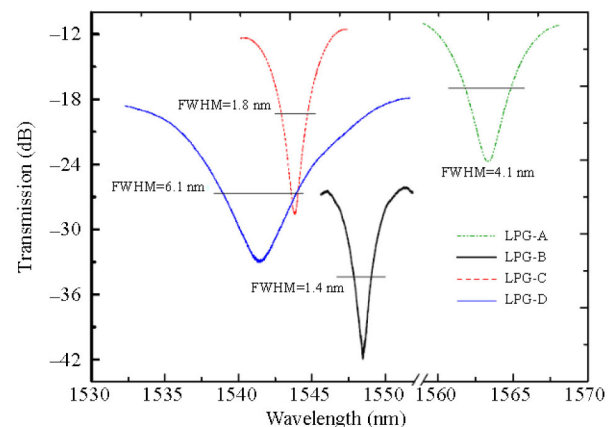


Fig. 4 Transmission spectra of gratings A, B, C, and D (the resonance wavelength lies at different spectral positions, but all present good strength; at the resonance wavelength, LPG-A presents a rejection of 14 dB, LPG-B shows a value of 11 dB, LPG-C reaches 17 dB, and LPG-D has a rejection of about 13 dB).

The periods of LPG-E and LPG-F were $A_E = 370 \mu\text{m}$ and $A_F = 380 \mu\text{m}$, respectively. With such parameters, the LPG-E resonance peak presented the maximum rejection of -11 dB at $\lambda_E = 1551.4 \text{ nm}$. LPG-F presented its minimum transmission at $\lambda_F = 1548.8 \text{ nm}$ with the rejection of -9.5 dB . The full widths at half maximum of the resonance spectral

bands are also indicated in Fig. 5, measuring 3.8 nm and 5.4 nm for the gratings LPG-E and LPG-F, respectively.

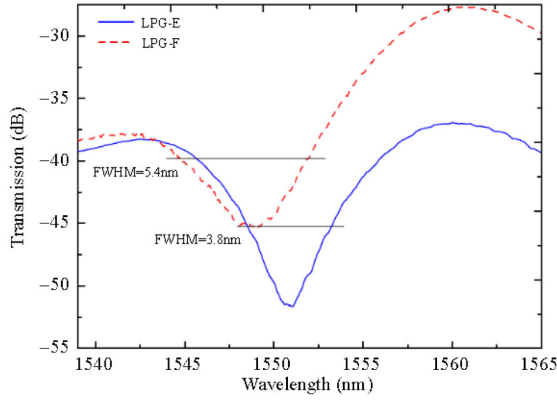


Fig. 5 LPG-E and LPG-F transmission spectra.

3. Strain and temperature characterization

Following the writing process, the next step of this work was to measure the characterizations of the LPG samples in relation to strain and temperature. Measurements were performed several times in order to achieve the improved statistical confidence of results. The experimental setup for investigating strain and temperature was almost the same as that used for writing the gratings and is schematically shown in Fig. 6. Two stages were used to hold and maintain the LPG stretched: one end of the fiber was fixed, and the other end was attached to the 13 g weight in order to obtain the same peak resonance wavelength achieved in the writing process. The temperature characterization of the LPG samples was done with the same setup. However, in such a case, the LPGs were fixed on a Peltier junction element. A thermocouple was used to monitor the temperature.

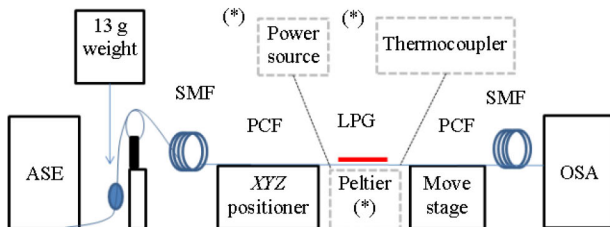


Fig. 6 Schematic of the experimental setup used for strain and temperature characterizations [the (*) symbol indicates the apparatus used only for the temperature test].

The resonant phase-matching condition for the coupling between the fundamental core and cladding modes of the long period grating is given by the well-known relation [24, 25]:

$$\lambda_{\text{res}} = \Lambda \left(n_{\text{eff}}^{\text{core}} - n_{\text{eff}}^{\text{clad},m} \right) \quad (1)$$

in which λ_{res} represents the peak resonance wavelength of the LPG in the transmission spectrum, Λ is the spatial pitch of the grating, $n_{\text{eff}}^{\text{core}}$ is the effective index of the core fundamental mode, and $n_{\text{eff}}^{\text{clad},m}$ is the effective index of the m th-order cladding mode. The $\Delta n_{\text{eff}} = (n_{\text{eff}}^{\text{core}} - n_{\text{eff}}^{\text{clad}})$ of the PCF is strongly dependent on the wavelength λ [3]. From the experimental curves in Fig. 4, the differences Δn_{eff} between core and cladding effective refractive indices for LPGs A, B, C, and D were calculated as 4.46×10^{-3} , 4.07×10^{-3} , 3.95×10^{-3} , and 3×10^{-3} , respectively. No other significant resonances were found in the measured spectra within the used wavelength range available. As the coupling of the fundamental mode to the first order cladding mode is the most privileged one for gratings written under the condition of normal incidence of the laser beam on the fiber, we concluded that in our case the observed stronger resonances were due to the coupling between the fundamental core mode and the LP₁₁ cladding mode [26].

Given the relationship stated in (1), one notes that when submitted to axial strain, considering temperature constant, the resonant wavelength will shift because the LPG period Λ increases. The refractive index of both core and cladding modes will also decrease due to the photoelastic effect. The shift dependence on strain is described by the derivative of λ_{res} in relation to strain [27]:

$$d\lambda_{\text{res}} / d\varepsilon = [(dn_{\text{eff}}^{\text{core}} / d\varepsilon) - (dn_{\text{eff}}^{\text{clad},m} / d\varepsilon)]\Lambda + (n_{\text{eff}}^{\text{core}} - n_{\text{eff}}^{\text{clad},m})d\Lambda / d\varepsilon. \quad (2)$$

In the same way, as the grating is submitted to temperature change, in a strain-constant configuration, the resonant wavelength shifts due to the thermal expansion or contraction of the grating

and also due to the thermo-optic effect. And the shift over temperature is described by the derivative of λ_{res} in relation to temperature [27]:

$$d\lambda_{\text{res}}/dT = [(dn_{\text{eff}}^{\text{core}}/dT) - (dn_{\text{eff}}^{\text{clad},m}/dT)]\Lambda + (n_{\text{eff}}^{\text{core}} - n_{\text{eff}}^{\text{clad},m})d\Lambda/dT. \quad (3)$$

In (2) and (3), ε is the axial strain, and T is the temperature to which the grating is subject. One also defines the elasto-optic and thermo-optic coefficients, respectively, as [14, 27]

$$\eta = (1/n)(dn/d\varepsilon) \quad (4)$$

$$\xi = (1/n)(dn/dT) \quad (5)$$

which defines the dependence of the PCF effective core and cladding refractive indices on strain. These coefficients are η_{core} and η_{clad} , respectively. A similar definition is used for the temperature dependence of the PCF effective core and cladding refractive indices on temperature, and the coefficients are ξ_{core} and ξ_{clad} , respectively.

3.1 Strain measurements

Figure 7 shows the behaviors of the resonance wavelengths of LPG-B, LPG-C, and LPG-D as the strain applied to the gratings increases. The standard deviation of data is also shown in the figure. Notice that the resonance wavelength shifts to lower values as the strain increases, showing that these LPGs have negative strain sensitivity. These results are consistent with data found in the literature for LPGs written in solid core PCFs [23, 27, 28]. For instance, the strain sensitivity of such LPG is determined by the elasto-optic coefficients η_{core} and η_{clad} and the period of the grating. An applied axial strain on the LPG affects the fundamental core and cladding modes in the fiber, because the size of waveguide changes, and so the group effective index changes [14]. Particularly, the group effective index of the cladding mode shows a highly dispersive behavior due to the existence of the air holes in the cladding, which strongly contributes to the negative value of the sensitivity calculated through (2).

Figure 8 shows the incremental change in the resonance wavelength in relation to the start position

in order to compare the grating sensitivities as a function of their period Λ . Calculated sensitivities of LPG-B, LPG-C, and LPG-D are $-5.86 \text{ pm}/\mu\varepsilon$, $-5.4 \text{ pm}/\mu\varepsilon$, and $-6.6 \text{ pm}/\mu\varepsilon$, respectively. The difference of only $10 \mu\text{m}$ between periods may not contribute much to distinguishing a significant trend in the experimental results, although an increase in sensitivity is perceived between LPG-B and LPG-D, which is accordance with the behavior described in (2). A comparison with results available in the literature shows that the sensitivity of LPG-D to strain is about 7 times larger than that reported in [28] ($-0.992 \text{ pm}/\mu\varepsilon$), about 8 times larger than that observed in a modal interferometer [29] ($-0.81 \text{ pm}/\mu\varepsilon$), and about 2.5 times larger than that reported in [30] ($-2.8 \text{ pm}/\mu\varepsilon$), which is made from a simple piece of photonic crystal fiber spliced to standard fibers.

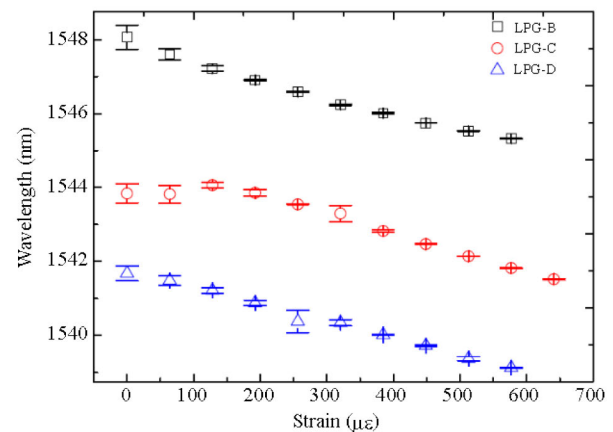


Fig. 7 LPG-B, LPG-C, and LPG-D resonance wavelengths as a function of the applied tensile strain (typical standard deviations were 6% for LPG-B, 7% for LPG-C, and 7% for LPG-D).

Although LPG-A was written with the same process, it represented a special case. The pitch of this grating was $\Lambda = 350 \mu\text{m}$, but presented a strong resonance wavelength with only three markings ($N=3$) of the CO_2 laser. In this way, LPG-A had a very short length of only 1.05 mm. Because of it, the tensile strain applied to LPG-A was in the range of 0 to $9 \mu\varepsilon$, whereas for LPG-B, LPG-C, and LPG-D, they were in the range of 0 to $600 \mu\varepsilon$. Figure 9 shows

the wavelength shift of LPG-A over strain. The statistical standard deviation of data for the reported measurements was 3.2%. From the linear best-fit of the resonance wavelength as a function of strain, the sensitivity of LPG-A was obtained as $-88 \text{ pm}/\mu\epsilon$. As a comparison, Wang *et al.* [22] fabricated an LPG by carving periodic and asymmetric grooves ($N=80$ and $\Lambda = 400 \mu\text{m}$) on one side of the optical fiber through repeated scanning of the CO₂ beam over the fiber surface. The resulted length was 3.2 cm, and the grating showed a sensitivity of $-102.89 \text{ nm}/\mu\epsilon$, which was about 17% higher than that of LPG-A.

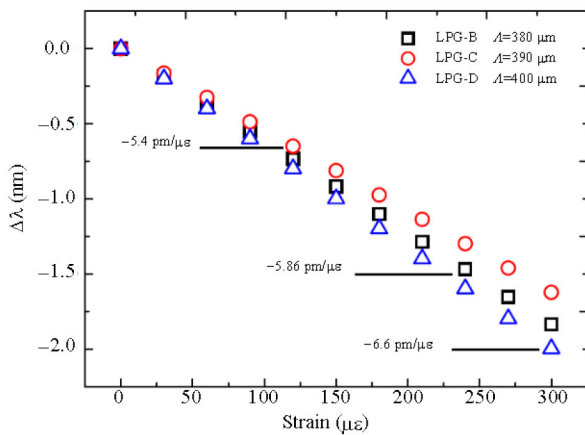


Fig. 8 Wavelength shift versus tensile strain for LPG-B, LPG-C, and LPG-D.

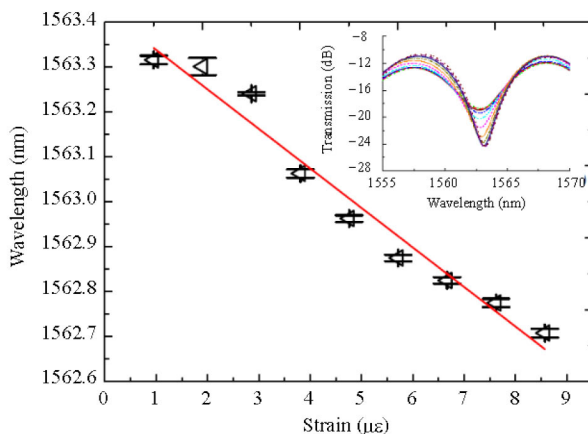


Fig. 9 Wavelength versus tensile strain for a very short grating, LPG-A (the inset shows the evolution of the resonance spectral band as the applied strain increases).

3.2 Temperature measurements

The temperature characterizations of LPG-E and

LPG-F were performed by heating the gratings with the Peltier junction element. The temperature range was set from 0 °C to 75 °C with a step of 5 °C. Room temperature was stable at 22 °C. The behavior of the incremental change in the resonance wavelength with temperature is plotted in Fig. 10.

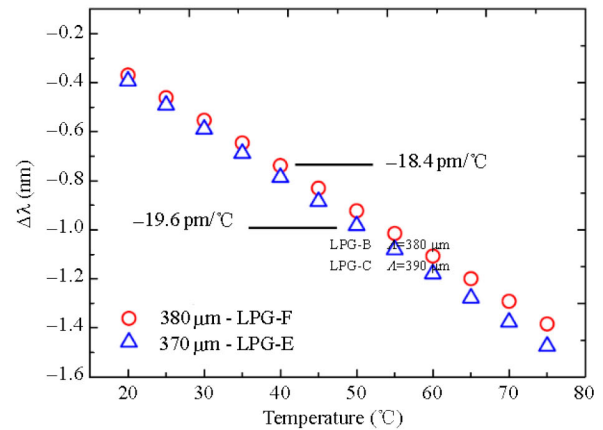


Fig. 10 Measured wavelength shifts of LPGs over temperature for different grating periods.

The curves show that the resonance wavelengths shift toward shorter wavelengths with an increase in temperatures, showing a negative temperature sensitivity. Equation (3) describes the sensitivity behavior over temperature. The temperature sensitivity is dependent on the thermo-optic coefficients of the pure silica core, $\xi_{\text{core}}=7.8 \times 10^{-6}/^\circ\text{C}$, the cladding, ξ_{clad} , and also on the waveguide properties and the period of the grating, which is affected by the thermal expansion coefficient of pure silica $\alpha = 4.1 \times 10^{-7}/^\circ\text{C}$. Just like the case of the strain sensitivity, the waveguide properties play again an important role in determining the positive or negative temperature sensitivity behavior. As n_{core} is always larger than n_{clad} , the negative contribution originates from the fact that the thermo-optic coefficient of the core, ξ_{core} , is smaller than the thermo-optic coefficient of the cladding ξ_{clad} for this type of PCF.

Both gratings exhibited a good linearity in their thermal responses in the considered range, as seen from the curves in Fig. 10. From the best-fitting calculation, the sensitivities of LPG-E and LPG-F

were $-19.6 \text{ pm}/^\circ\text{C}$ and $-18.4 \text{ pm}/^\circ\text{C}$, respectively. One also notes that the slope of the curve becomes larger as the period decreases. Shu *et al.* [31] have also demonstrated LPGs with periods between $240 \text{ }\mu\text{m}$ and $500 \text{ }\mu\text{m}$, whose sensitivity to temperature was higher for shorter periods, in accordance with the values shown by the gratings of this work. The spectral measurements over temperature were performed three times for each grating in order to improve statistical confidence. A comparison to data available in the literature showed that LPG-E presented, for instance, a similar temperature sensitivity ($-19.6 \text{ pm}/^\circ\text{C}$) as that found in LPGs written in pure silica PCF by CO_2 laser ($-21.51 \text{ pm}/^\circ\text{C}$) [28], but different from the sensitivity ($-10.9 \text{ pm}/^\circ\text{C}$) found by Zhu *et al.* [32] for LPGs in photonic crystal fiber by the use of focused pulses of a CO_2 laser and a periodic stress relaxation technique without geometrical deformation and elongation of the fiber.

4. Conclusions

In this paper, strain and temperature characteristics of long period fiber gratings written in a pure silica solid, not hydrogenated, core photonic crystal fiber with CO_2 laser were investigated. Gratings were written with different numbers of points N and periods A . Regarding the applied tensile strain testing, it was observed that there was a shift of the resonance wavelength to shorter values when the strain increased. The obtained strain sensitivities were slightly larger than those obtained in [28] and also larger than the strain sensitivities by the use of other measurement techniques in [29]. A very short LPG ($L=1 \text{ mm}$), with only three points marked by the CO_2 laser pulses in the fiber presented a high strain of $-88 \text{ pm}/\mu\text{e}$, demonstrating the possibility of compact and high sensitive strain sensors.

The temperature tests also showed that the sensitivities of the two investigated samples of LPGs were negative: as the temperature increased, the

resonance wavelength decreased. The temperature sensitivity obtained with LPG-E was $-19.6 \text{ pm}/^\circ\text{C}$ and can possibly be used for the fabrication of high-resolution temperature sensors. All fabricated gratings showed the good performance and similar values, as compared to the previous results found in the literature, in terms of strain and temperature sensitivities. The improvement in the laser setup, particularly to make the pulses hit the fiber on all sides (front and back), providing a homogenous heating distribution on the fiber surface, is a valuable effort for obtaining better quality gratings for sensing applications in the future.

Acknowledgment

The authors would like to thank CAPES (AUX-PE_PRODEFESA 1880/2008), Santa Catarina State University (UDESC), CNPq (FOTONICOM Project), FAPESC (PAP/UDESC 3447/2013), and Prof. Hypolito José Kalinowski of UTFPR by valuable discussions.

Open Access This article is distributed under the terms of the Creative Commons Attribution License which permits any use, distribution, and reproduction in any medium, provided the original author(s) and source are credited.

References

- [1] P. S. J. Russell, "Photonic-crystal fibers," *Journal of Lightwave Technology*, 2006, 24(12): 4729–4749.
- [2] A. C. Sodré Junior, "Recent progress and novel applications of photonic crystal fibers", *Reports on Progress in Physics*, 2010, 73(2): 1–21.
- [3] T. Birks, J. C. Knight, and P. S. Russell, "Endlessly single-mode photonic crystal fiber," *Optics Letters*, 1997, 22(13): 961–963.
- [4] K. Nakajima, K. Hogari, J. Zhou, K. Tajima, and I. Sankawa, "Hole-assisted fiber design for small bending and splice losses," *IEEE Photonics Technology Letters*, 2003, 15(12): 1737–1739.
- [5] J. Fatome, C. Fortier, T. N. Nguyen, T. Chartier, F. Smektala, K. Messaad, *et al.*, "Linear and non-linear characterization of chalcogenide photonic crystal fibers," *Journal of Lightwave Technology*, 2009, 27(11): 1707–1715.

- [6] J. M. Pottage, D. M. Bird, T. D. Hedley, T. A. Birks, J. C. Knight, P. S. J. Russell, *et al.*, “Robust photonic band gaps for hollow core guidance in PCF made from high index glass,” *Optics Express*, 2003, 11(22): 2854–2861.
- [7] C. Cordeiro, E. M. dos Santos, C. H. Brito Cruz, C. J. de Matos, and D. S. Ferreira, “Lateral access to the holes of photonic crystal fibers—selective filling and sensing applications,” *Optics Express*, 2006, 14(18): 8403–8412.
- [8] W. Qian, C. Zhao, C. Chan, L. Hu, T. Li, W. Wong, *et al.*, “Temperature sensing based on ethanol-filled photonic crystal fiber modal interferometer,” *IEEE Sensors Journal*, 2012, 12(8): 2593–2597.
- [9] J. Eggleton, P. S. Westbrook, C. A. White, C. Kerbage, R. S. Windeler, and G. L. Burdge, “Cladding-mode-resonances in air-silica microstructure optical fibers,” *Journal of Lightwave Technology*, 2000, 18(8): 1084–1100.
- [10] Y. Rao, Y. Wang, Z. Ran, and T. Zhu, “Novel fiber-optic sensors based on long-period fiber gratings written by high-frequency CO₂ laser pulses,” *Journal of Lightwave Technology*, 2003, 21(5): 1320–1327.
- [11] Y. Wang, “Review of long period fiber gratings written by CO₂ laser,” *Journal of Applied Physics*, 2010, 108(8): 081101-1–081101-18.
- [12] Y. Kondo, K. Nouchi, T. Mitsuyu, M. Watanabe, P. G. Kazansky, and K. Hirao, “Fabrication of long-period fiber gratings by focused irradiation of infrared femtosecond laser pulses,” *Optics Letters*, 1999, 24(10): 646–648.
- [13] K. Shima, K. Himeno, T. Sakai, S. Okude, A. Wada, and R. Yamauchi, “A novel temperature-insensitive long-period fiber grating using a boron-codoped-germanosilicate-core fiber,” in *Conference on Optical Fiber Communication*, Dallas, TX, pp. 347–348, 1997.
- [14] C. Zhao, L. Xiao, J. Ju, M. Demokan, and W. Jin, “Strain and temperature characteristics of a long-period grating written in a photonic crystal fiber and its application as a temperature-insensitive strain sensor,” *Journal of Lightwave Technology*, 2008, 26(2): 220–227.
- [15] A. M. Vengsarkar, P. J. Lemaire, J. B. Judkins, V. Bhatia, T. Erdogan, and J. E. Sipe, “Long period fiber gratings as band-rejection filters,” *Journal of Lightwave Technology*, 1996, 14(1): 58–65.
- [16] Z. Wang, K. S. Chiang, and Q. Liu, “Microwave photonic filter based on a circulating cladding mode in a fiber ring resonator,” *Optics Letters*, 2010, 35(5): 769–771.
- [17] A. M. Vengsarkar, J. R. Pedrazzani, J. B. Judkins, P. J. Lemaire, N. S. Bergano, and C. R. Davidson, “Long period fiber grating based gain equalizers,” *Optics Letters*, 1996, 21(5): 336–338.
- [18] M. Yang, Y. Li, and D. Wang, “Long period fiber gratings fabricated by use of defocused CO₂ laser beam for polarization-dependent loss enhancement,” *Journal of Optical Society of America*, 2009, 26(6): 1203–1208.
- [19] Y. Wang, D. Wang, W. Jin, Y. Rao, and G. Peng, “Asymmetric long period fiber gratings fabricated by use of CO₂ laser to carve periodic grooves on the optical fiber,” *Applied Physics Letters*, 2006, 89(15): 151105-1–151105-3.
- [20] Y. Wang, W. Jin, and D. Wang, “Strain characteristics of CO₂ laser-carved long period fiber gratings,” *IEEE Journal of Quantum Electronics*, 2007, 43(2): 101–108.
- [21] J. M. P. Coelho, M. C. Nespereira, M. Abreu, and J. M. Rebordão, “Modeling refractive index change in writing long-period fiber gratings using mid-infrared laser radiation,” *Photonic Sensors*, 2013, 3(1): 67–73.
- [22] Y. Wang, C. Liao, X. Zhong, J. Zhou, Y. Liu, and Z. Li, “Long period fiber gratings writing in photonic crystal fiber by use of CO₂ laser,” *Photonic Sensors*, 2013, 3(3): 193–201.
- [23] Y. Zhu, P. Shum, J. H. Chong, M. Rao, and C. Lu, “Deep notch, ultracompact long period grating in a large-mode-area photonic crystal fiber,” *Optics Letters*, 2003, 28(24): 2467–2469.
- [24] V. Bhatia and A. M. Vengsarkar, “Optical fiber long-period grating sensors,” *Optics Letters*, 1996, 21(9): 692–694.
- [25] V. Bhatia, “Applications of long period gratings to single and multiparameter sensing,” *Optics Express*, 1999, 4(11): 457–466.
- [26] K. Morishita and Y. Miyake, “Fabrication and resonance wavelengths of long-period gratings written in a pure-silica photonic crystal fiber by the glass structured change,” *Journal of Lightwave Technology*, 2004, 22(2): 625–630.
- [27] X. Shu, L. Zhang, and I. Bennion, “Sensitivity characteristics of long-period fiber gratings,” *Journal of Lightwave Technology*, 2002, 20(2): 255–266.
- [28] Q. Huang, Y. Yu, Z. Ou, X. Chen, J. Wang, P. Yan, *et al.*, “Refractive index and strain sensitivities of a long period fiber grating,” *Photonic Sensors*, 2014, 4(1): 92–96.

- [29] G. Kim, T. Cho, K. Hwang, K. Lee, K. S. Lee, Y. G. Han, *et al.*, "Strain and temperature sensitivities of an elliptical hollow-core photonic bandgap fiber based on sagnac interferometer," *Optics Express*, 2009, 17(4): 2481-2486.
- [30] J. Villatoro, V. Finazzi, V. P. Minkovich, V. Pruneri, and G. Badenes, "Temperature-insensitive photonic crystal fiber interferometer for absolute strain sensing," *Applied Physics Letters*, 2007, 91(9): 091109.
- [31] X. Shu, T. Allsop, B. Gwandu, L. Zhang, and I. Bennion, "High temperature sensitivity of long period gratings in B-Ge codoped fiber," *Photonics Technology Letters*, 2001, 13(8): 818-820.
- [32] Y. Zhu, P. Shum, H. W. Bay, M. Yan, X. Yu, J. Hu, *et al.*, "Strain-insensitive and high-temperature long-period gratings inscribed in photonic crystal fiber," *Optics Letters*, 2005, 30(4): 367-369.